Guo-xun Chang, Ke-feng Ren*, Yi-xiu Zhao, Yi-xin Sun and Jian Ji*

Modulation of cell behaviors by electrochemically active polyelectrolyte multilayers

Abstract: In addition to the topographical features and chemical properties of substrates, the mechanical properties are known as a vital regulator of cellular processes such as adhesion, proliferation, and migration, and have received considerable attention in recent years. In this work, electrochemical redox multilayers made of ferrocene-modified poly(ethylenimine) (PEI-Fc) and deoxyribonucleic acid (DNA) with controlled stiffness were used to investigate the effects of the mechanical properties of multilayers on fibroblast cell (NIH/3T3) behaviors. Redox PEI-Fc plays an essential role in inducing swelling in multilayers under an electrochemical stimulus, resulting in distinct changes in the stiffness of the multilayers. The Young's modulus varied from 2.05 to 1.07 MPa for the (PEI-Fc/DNA) multilayers by changing the oxidation time of the electrochemical treatment. We demonstrated that the adhesion, proliferation, and migration of fibroblast cells depended on the multilayers' stiffness. These results indicate that cell behaviors can be precisely controlled by electrochemical treatment, which provides a new way to prepare thin films with tunable mechanical properties with potential biomedical applications.

Keywords: cell behaviors; electrochemical oxidation; ferrocene; stiffness; stimuli-responsive multilayers.

DOI 10.1515/epoly-2014-0075
Received April 20, 2014; accepted May 16, 2014; previously published online June 14, 2014

1 Introduction

The layer-by-layer (LBL) deposition of polyelectrolytes onto solid substrates is a universal and easy-to-perform way to fabricate versatile nanocomposite thin films with tunable surface properties (1–6). The mechanical properties of multilayers can be changed through a variety of methods such as the temperature (7), pH (8), ionic strength (9), electromagnetic fields, and radiation (10). With the use of stimuli-responsive materials in the study of multilayers, stimuli-responsive multilayers, which can adjust the nanostructures, elastic modulus, and hydrophilicity of the materials, can be prepared and obtained. The numerous functions that can be performed by stimuli-responsive multilayers have attracted considerable interest from researchers (11–14). Compared to other responses, electrochemical stimuli can tune more mildly and reversibly not only the properties of multilayer films but also the function of the multilayers topically by changing the voltage without causing any effect on the structure and function of the ambient molecules, cells, and tissues (15, 16). Because of those advantages, the method of electrochemically active polyelectrolyte multilayers has been applied in the field of biosensing (17) and drug-controlled release (18).

Electrochemically active polyelectrolyte multilayers bearing redox groups such as ferrocene (19), viologen (20), and osmium bipyridyl complex (21) have been used for constructing biomaterials for several years now. However, all these studies were focused on the material science perspective; they merely made an in-depth research at the cellular level (22, 23). It could be very interesting to prepare electrochemically active polyelectrolyte multilayers (ranging from nanometers to micrometers in thickness) and investigate their influences on cell behaviors, since there are great potential applications for such thin films for biomedical surface modification. It is well known that substrate stiffness has strong effects on almost all kinds of cell behaviors (24–26). Although the stiffness optima for different kinds of cells vary widely, it is generally true that cells display a spreading preference for stiffer substrates and prefer to migrate toward the stiffer regions of a substrate. The possibility of varying the mechanical stiffness by proton exchange membrane (PEM) film deposition would be a good way to control the cellular processes.

Ferrocene is an organic-metal compound. It is stable at room temperature and has been widely used in

***Corresponding authors: Ke-feng Ren and Jian Ji,** MOE Key Laboratory of Macromolecule Synthesis and Functionalization, Department of Polymer Science and Engineering, Zhejiang University, Hangzhou, China, Tel./Fax: +86 571 87953729, e-mail: Renkf@zju.edu.cn, Jijian@zju.edu.cn
Guo-xun Chang, Yi-xiu Zhao and Yi-xin Sun: MOE Key Laboratory of Macromolecule Synthesis and Functionalization, Department of Polymer Science and Engineering, Zhejiang University, Hangzhou, China

electrochemical fields (27–29). The transformation of Fe(II) and Fe(III) in the multilayers results in the swelling phenomenon, which causes the changes in the stiffness of the multilayers (30). So, in our previous study (31, 32), we used ferrocenecarboxaldehyde and poly(ethyleneimine) (PEI) to synthesize ferrocene-modified poly-(ethylenimine) (PEI-Fc). Ferrocene-modified poly-(ethylenimine) and deoxyribonucleic acid (DNA) were chosen to form the polyelectrolyte multilayers. The stiffness of the (PEI-Fc/DNA) multilayers decreases when the ferrocene groups undergo electrochemical redox treatment.

In this study, we further investigated the cell behaviors of the (PEI-Fc/DNA) multilayers. The stiffness of the (PEI-Fc/DNA) multilayers was controlled by electrochemical treatment with different oxidation times, from 0 to 20 min. The electrochemical properties of the multilayers were investigated by cyclic voltammetry. We learned that the stiffness of (PEI-Fc/DNA) multilayers with 15 bilayers can be tuned from 2.05 to 1.07 MPa. Moreover, we found that the changes in stiffness played an important role in the fibroblast cell adhesion, proliferation, and migration.

2 Materials and methods

2.1 Materials

Poly(ethyleneimine) (PEI, branched, molecular weight 25,000) and ferrocene-carboxaldehyde (98%) were purchased from Sigma-Aldrich. PEI-Fc (10 mol% grafting density of Fc) was synthesized as previously reported by our group (19, 29). DNA (fish sperm, sodium salt) and phosphate buffered saline (PBS) were purchased from Sangon Biotech (Shanghai, China). Glutaraldehyde solution (25%) was purchased from Sinopharm Chemical Reagent (Shanghai, China). Dulbecco's Modified Eagle's Medium (DMEM), fetal bovine serum (FBS, Gibco, NY, USA), 0.25% trypsin-EDTA solution, and penicillin and streptomycin (P/S) were purchased from Future Biochemical-Tech (Shanghai, China). ITO glass was purchased from Zhuhai Kaivo Electronic Components (Zhuhai, China). All of the chemicals and solvents were of analytical grade.

2.2 Preparations for the $(PEI\text{-}Fc/DNA)_{15}$ multilayers

ITO glass coverslips (8×17 mm^2) were cleaned with acetone solution for 15 min and then with ethanol solution for 15 min, rinsed thoroughly with deionized water, and finally blow dried with a stream of nitrogen. The $(PEI\text{-}Fc/DNA)_{15}$ multilayers were built up by alternately immersing the substrate in PEI-Fc and DNA solutions (both at 1 mg/ml in PBS). Sequential adsorption of polyelectrolytes was performed by hand dipping for 10 min in each polyelectrolyte, followed by rinsing in PBS for 1 min each. Cross-linking of the multilayers was performed in glutaraldehyde solution (0.1%, PBS at pH 7.4). Briefly, the multilayers were incubated in glutaraldehyde solution for 3 min. Rinsing steps were performed with PBS for 1 h. Then the multilayers were electrochemically treated at different oxidation times of 0, 2, 5, 10, and 20 min. The scan voltammetry was 0.5 V.

2.3 Electrochemical measurements

Cyclic voltametric and amperometric measurements were performed with a conventional three-electrode potentiostatic system. The equipment was a CHI-660D electrochemistry workstation (Shanghai Chen Hua, Shanghai, China). A three-electrode cell was used with a saturated KCl electrode as the reference, a platinum flake as the counter, and the ITO glass with the multilayers as the working electrode. PBS solution (pH 7.4) was used as the electrolyte. In the electrochemical treatment process, amperometric measurements were used to oxidize the $(PEI\text{-}Fc/DNA)_{15}$ multilayers, and cyclic voltammetry was used to characterize the electrochemical properties of the multilayers.

2.4 Characterization of the $(PEI\text{-}Fc/DNA)_{15}$ multilayers

The top images and the *Z*-axis view of the $(PEI\text{-}Fc/DNA)_{15}$ multilayers were acquired by confocal laser scanning microscopy (CLSM), which was performed with a Leica TCS SP5 confocal setup mounted on a Leica DMI 6000 CS inverted microscope (25 mW argon laser; Leica Microsystems, Wetzlar, Germany), which was operated using the Leica Application Suite Advanced Fluorescence (LAS AF) program. One layer of $PEI^{\text{-FITC}}$ was introduced into the multilayers. To excite the fluorophore fluorescent isothiocyanate (FITC), confocal illumination was provided by an argon-ion laser at 488 nm. The surface morphologies of the films deposited on the ITO slides were monitored by atomic force microscopy (AFM; SPA400, Seiko, Japan) by tapping mode in air. The root-mean-square (RMS) roughness values were obtained using the XEI software (Seiko, Japan). All measurements were carried out under room temperature. The stiffness of the films was measured by

a Nano Indenter G200 instrument (Agilent). All experiments were performed in a liquid environment.

2.5 Cell culture

Mouse embryonic fibroblast NIH/3T3 cells were used as model cells. The cells were maintained in a regular growth medium consisting of high-glucose DMEM (Gibco, USA), supplemented with 10% FBS (Gibco) and 1 IU/ml of P/S, and cultured at 37°C in a humidified atmosphere containing 5% CO_2. The culture medium was changed every 3 days. Cells were grown to approximately 80% confluence and then trypsinized for passage or for cell experiments.

2.6 Cell adhesion and proliferation

In the cell adhesion assay, the cells were seeded on the multilayer surfaces (electrochemical treatment for 0, 2, 5, 10, and 20 min at 500 mV) at a density of $1\times10^4/cm^2$. Four hours later, the ITO slides were rinsed three times with PBS. The cells were fixed in paraformaldehyde solution (3.7%, in PBS). The cells were then stained with nuclei (1:100, 4′, 6-diamidina-2-phenylin, D9542; Sigma) and F-actin (1:600, rhodamine-phalloidin, P1951; Sigma). All the ITO slides were fixed onto coverslips with an antifade reagent (ProLong Gold, Invitrogen) and viewed under a fluorescence microscope (Axio-vert 200 M, Zeiss Germany) with 10× objectives. The cell densities were determined by using the ImageJ software.

For the cell proliferation assay, the cell seeding and culturing methods were similar to those described for the cell adhesion assay. After culturing for 12, 24, 48, and 72 h, the cells were then washed three times with PBS and fixed with paraformaldehyde solution (3.7%, in PBS). To quantify cell proliferation, the cells were stained with nuclei and F-actin. Cell densities were determined by analyzing the fluorescence images using the ImageJ software.

2.7 Cell migration

Before the cell culture process, the multilayers were sterilized under UV light for 30 min. The cells were seeded ($5\times10^3/cm^2$) on the multilayers that were treated at different oxidation times. Approximately 12 h after the cell seeding, the cell migration was recorded in situ by using a time-lapse, phase-contrast microscope (IX81, Olympus) equipped with an incubation chamber. The temperature and CO_2 level were maintained at 37°C and 5%, respectively. Video and image analysis were performed with the ImageJ software and a manual tracking method. From each condition, the x/y coordinates of the cells were noted for 20 cells at 10-min intervals and then normalized to a common point of origin. Total distance traveled was calculated as the cumulative distance regardless of the direction of movement.

2.8 Statistical analysis

The data were expressed as the mean±standard deviation. The statistical significance between groups was determined by one-way analysis of variance using the Origin software.

3 Results and discussion

3.1 Preparation of the (PEI-Fc/DNA) LBL multilayers

The PEI-Fc was synthesized according to a published procedure (19). The grafting density of ferrocene on PEI was 10 mol%. As DNA has an excellent biocompatibility and is commercially available, we chose it as the anionic polyelectrolyte. An alternate adsorption of PEI-Fc and DNA was conducted as discussed in a previous report (31). The silicon or ITO substrates were immersed in a 1 mg/ml solution of PEI-Fc, rinsed, and then immersed in a DNA solution of the same concentration.

The sequential buildup of PEI-Fc/DNA multilayers characterized by UV-Vis spectrophotometry and Quartz Crystal Microbalance with Dissipation monitoring technique (QCM-D) was reported previously by our group (28). Those observations suggested a successful fabrication of hydrogel-like (PEI-Fc/DNA) multilayers. The thickness in dry state of the multilayer was monitored by a spectroscopic ellipsometer on silicon wafers, which exhibited exponential growth with a thickness of 420 nm for five bilayers. The $(PEI\text{-}Fc/DNA)_{15}$ multilayers loaded with FITC-labeled PEI were investigated by CLSM (Figure 1). A green fluorescent band indicated that PEI could diffuse throughout the (PEI-Fc/DNA) multilayers. Based on the CLSM measurement, the thickness of the $(PEI\text{-}Fc/DNA)_{15}\text{-}PEI^{\text{-FITC}}$ film was ~3 μm.

Figure 1 Vertical section image of $(PEI\text{-}Fc/DNA)_{15}\text{-}PEI^{\text{-FITC}}$ in the wet state obtained by CLSM observation.

3.2 Electrochemical oxidation and cyclic voltammetry characterization of the $(PEI\text{-}Fc/DNA)_{15}$ multilayers

Ferrocene is a redox group known for its quasi-reversible oxidation, which has been widely used for developing redox-active organic materials (33–35). Recently, we reported that the stiffness of the (PEI-Fc/DNA) multilayers can be controlled by electrochemical oxidation. The electrochemical swelling of the multilayers was driven by a change in charge densities within the film. When the redox state of ferrocene groups in the multilayers was changed, counterions diffused to compensate the increase of positive charge within the multilayers and provided electroneutrality. This increase in osmotic pressure was balanced by elastic multilayer deformations that led to the swelling behavior. In addition, electrostatic repulsion combined with different electrostatic bindings of polycations and polyanions could also be a factor.

In this work, an electrochemical workstation was used to electrochemically oxidize the $(PEI\text{-}Fc/DNA)_{15}$ multilayers. The $(PEI\text{-}Fc/DNA)_{15}$ multilayers oxidized at 0, 2, 5, 10, and 20 min were obtained under an applied oxidation potential of 0.5 V. As shown in Figure 2, along with the oxidation times, the color of the $(PEI\text{-}Fc/DNA)_{15}$ multilayers gradually changed from light to dark yellow, which means that the ferrocene groups within the multilayers were oxidized continuously.

In the cyclic voltammograms recorded from the $(PEI\text{-}Fc/DNA)_{15}$ multilayers, cyclic voltammetry (CV) curve could be used to estimate the degree of oxidation. Figure 3 shows the CV curves that were acquired as a function of different oxidation times. For the original $(PEI\text{-}Fc/DNA)_{15}$ multilayers, the figure shows a well-defined and nearly reversible CV peak pair at about 0.44 V vs. the saturated calomel electrode (SCE). However, with the increase in oxidation time of the $(PEI\text{-}Fc/DNA)_{15}$ multilayers, the response of the CV was suppressed. The peak current of the $(PEI\text{-}Fc/DNA)_{15}$ multilayers decreased exponentially with the increase in oxidation time, suggesting that different degrees of oxidation had been achieved.

To monitor the morphological changes caused by the oxidation of the multilayers, AFM was used. Surface structures that formed at various oxidation times at a voltage

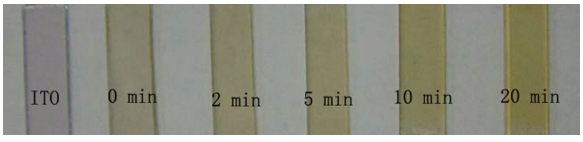

Figure 2 Color changes of the $(PEI\text{-}Fc/DNA)_{15}$ multilayers at different oxidation times of the electrochemical treatments.

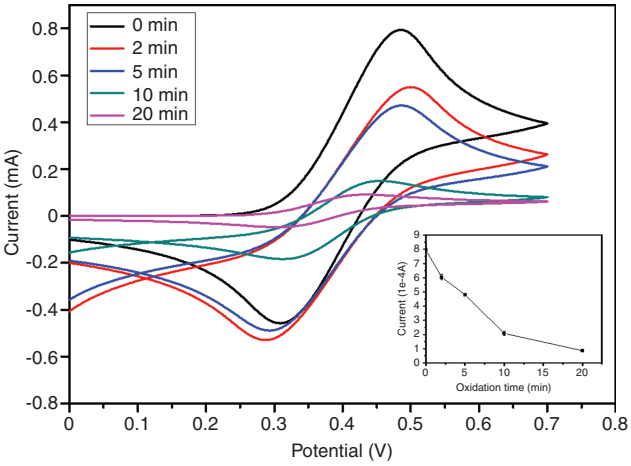

Figure 3 Cyclic voltammograms of the $(PEI\text{-}Fc/DNA)_{15}$ multilayers washed with PBS (pH 7.0) and electrochemically treated at different oxidation times (scan rate 0.1 V/s). Inset: Anodic peak current as a function of the oxidation time.

of 0.5 V are shown in Figure 4. Despite the different oxidation times, the multilayers were smooth. No breakdown of the multilayers was found throughout the experiments. The RMS roughness of the $(PEI\text{-}Fc/DNA)_{15}$ multilayers with oxidation times of 0, 2, 5, 10, and 20 min was 1.23, 1.12, 1.2, 1.31, and 1.18 nm, respectively. Very flat surfaces were observed, and the electrochemical treatment did not change the surfaces. We then investigated the change in elastic modulus of the $(PEI\text{-}Fc/DNA)_{15}$ multilayers under electrochemical treatments. Table 1 shows the Young's modulus and the RMS roughness of $(PEI\text{-}Fc/DNA)_{15}$ multilayers at different oxidation times. For the multilayers that were not electrochemically treated, the elastic modulus was measured to be 2.05±0.20 MPa. The stiffness of the multilayers decreased with the increase in oxidation time. That is, a given stiffness could be obtained by controlling the oxidation time. After 2 min of electrochemical treatment, the elastic modulus of the multilayers was slightly decreased to 1.9±0.32 MPa, whereas at 20 min, it was 1.07±0.15 MPa.

Cell adhesion is the first and a very important step in cell-substrate interactions. In order to assess whether cells are sensitive to the various rigidity levels provided by the electrochemical treatment of the $(PEI\text{-}Fc/DNA)_{15}$ multilayers, we carried out a cell adhesion experiment. Figure 5 shows the cells that were stained with F-actin and nucleus, and cultured on the $(PEI\text{-}Fc/DNA)_{15}$ multilayers at different oxidation times. Distinct cell spreading and shapes were observed between the different multilayers. Whereas many cells spread very well on the multilayers before the electrochemical treatment, the cell spreading area decreased as the oxidation time increased, as shown

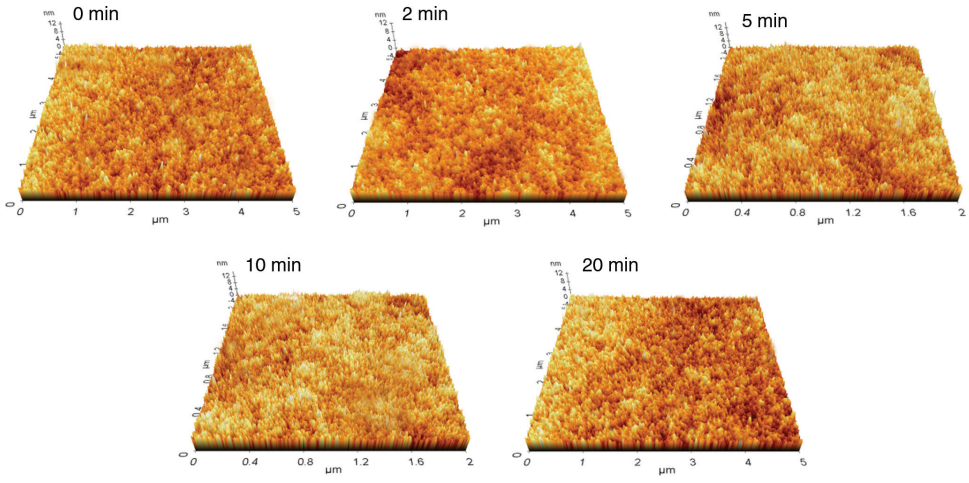

Figure 4 AFM images of the surface structures of the $(PEI\text{-}Fc/DNA)_{15}$ multilayers at different oxidation times at a voltage of 0.5 V.

Table 1 Young's modulus and RMS roughness of the $(PEI\text{-}Fc/DNA)_{15}$ multilayers at different oxidation times.

Oxidation time (min)	RMS roughness (nm)	Young's modulus (MPa)
0	1.23±0.08	2.05±0.20
2	1.12±0.12	1.90±0.32
5	1.20±0.15	1.63±0.29
10	1.31±0.11	1.42±0.42
20	1.18±0.16	1.07±0.15

Cell adhesion and proliferation on the $(PEI\text{-}Fc/DNA)_{15}$ multilayers.

in Figure 6F. Cells on the stiffer multilayers appeared to be well spread and adhered, and long filopodia could be clearly observed. Conversely, cells on the softer multilayers displayed a round morphology and were poorly spread. The cell spreading area was generally assumed to give an indication of cell adhesion. The cell spreading area of unoxidized multilayers reached 1600 μm^2/cell and slightly decreased when the multilayers were oxidized for 2 min. A distinct decrease in the cell spreading area appeared when the oxidation time reached 10 min. After that, however, the cell spreading area did not change much. The cell spreading area of the unoxidized multilayers was four times larger of the fully oxidized multilayers, which indicates that the electrochemical oxidation of multilayers can splendidly regulate and control cell adhesion.

We further investigated how the electrochemical oxidation of multilayers affected the proliferation of fibroblast cells. Figure 7 shows the number of cells and the

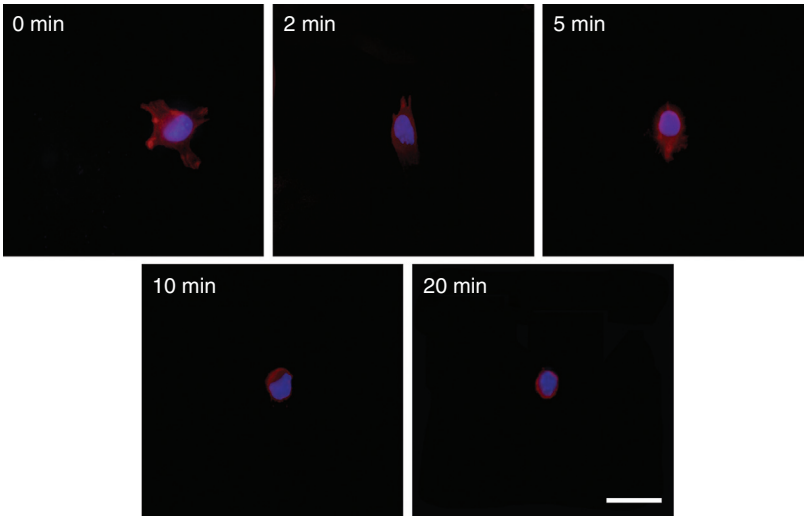

Figure 5 Immunofluorescence images of the cells [stained with F-actin (red) and nuclei (blue)] on the $(PEI\text{-}Fc/DNA)_{15}$ multilayers at different oxidation times. Scale bar is 20 μm.

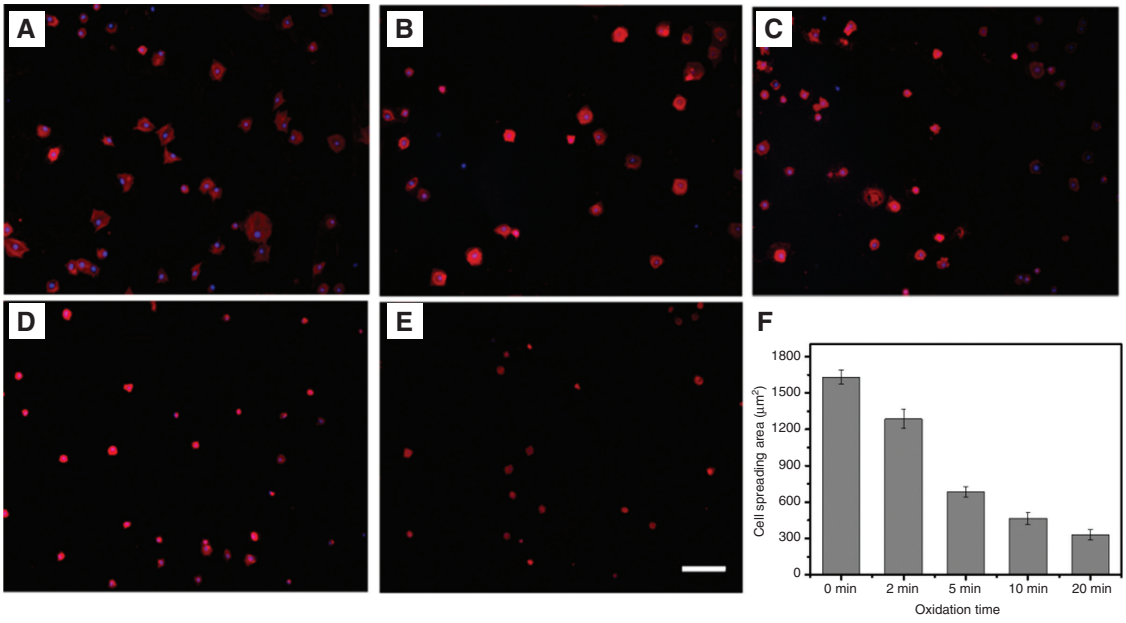

Figure 6 Immunofluorescence images of the cells [stained with F-actin (red) and nuclei (blue)] on the $(PEI\text{-}Fc/DNA)_{15}$ multilayers at different oxidation times. (A–E) The multilayers at various oxidation times of 0, 2, 5, 10, and 20 min. Scale bar is 200 μm. (F) Cell spreading area of the $(PEI\text{-}Fc/DNA)_{15}$ multilayers at different oxidation times.

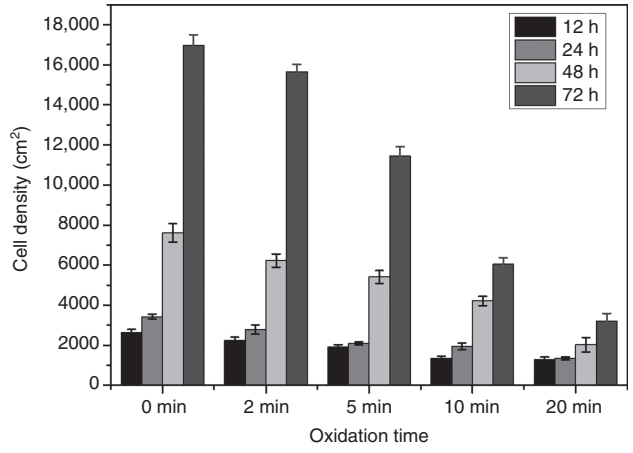

Figure 7 The cell proliferation assay. Cell density of the $(PEI\text{-}Fc/DNA)_{15}$ multilayers at different oxidation times after being cultured for 12, 24, 48, and 72 h. The number of cells was calculated from at least 10 images based on the fluorescence images using the ImageJ software.

cell proliferation on the $(PEI\text{-}Fc/DNA)_{15}$ multilayers. For all the multilayers, the number of cells presented a pattern of exponential growth along with the time. One can observe that there was a higher cell proliferation rate on the stiff $(PEI\text{-}Fc/DNA)_{15}$ multilayers than on the soft ones. Cell density on unoxidized multilayers was nearly four times bigger as compared to fully oxidized multilayers (20 min), which shows that the electrochemical oxidation of $(PEI\text{-}Fc/DNA)_{15}$ multilayers, namely, the stiffness, strongly affected the proliferation of cells.

3.3 Cell migration in the $(PEI\text{-}Fc/DNA)_{15}$ multilayers

Time-lapse video analysis of NIH/3T3 cells on differently oxidized $(PEI\text{-}Fc/DNA)_{15}$ multilayers not only can corroborate the notable differences in cell morphology and spreading, but also reveal the contrasting differences in movement between the various oxidized $(PEI\text{-}Fc/DNA)_{15}$ multilayers. Graphic representations of the cellular movements revealed an erratic and random behavior with frequent directional changes for cells in the multilayers oxidized at various times. Figure 8 shows the cell migration behaviors in the $(PEI\text{-}Fc/DNA)_{15}$ multilayers at different oxidation times. The cells on 0–min-oxidized multilayers travelled significantly longer distances (492 μm) at an average rate of 0.8 μm/min and displayed "step-like" movements, compared to the movements (403 μm at 0.63 μm/min) observed on 2-min-oxidized multilayers. Although the cells on 5-min-oxidized multilayers were also somewhat erratic, they changed direction less frequently and traveled more slowly (154 μm at 0.35 μm/min) than those on 0- and 2-min-oxidized multilayers. The cells on 10-min-oxidized multilayers traveled

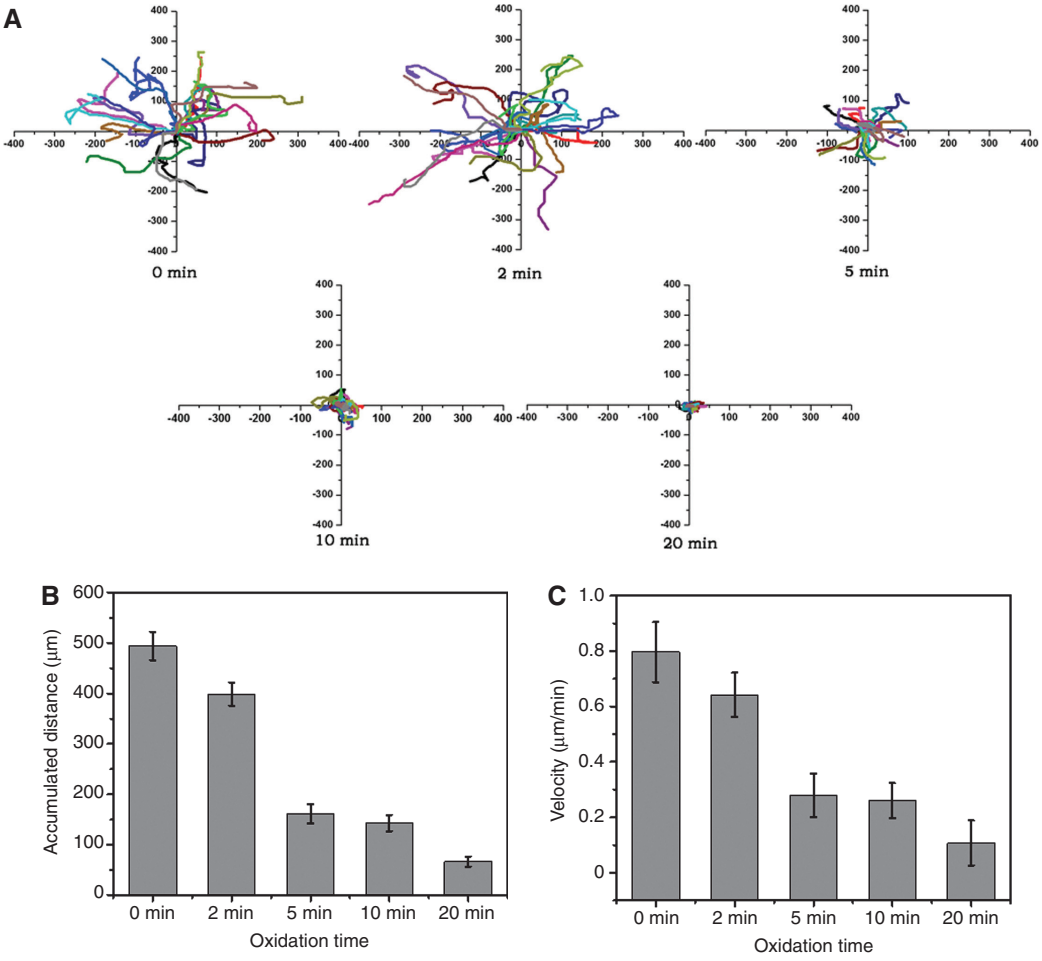

Figure 8 (A) Cell migration trajectories in the $(PEI\text{-}Fc/DNA)_{15}$ multilayers at different oxidation times. The cells were randomly tracked for 12 h after being cultured for 12 h at a seeding density of $5\times10^3/cm^2$. (B) Accumulated cell migration distance in the $(PEI\text{-}Fc/DNA)_{15}$ multilayers functioning at different oxidation times. (C) Cell migration velocity in the $(PEI\text{-}Fc/DNA)_{15}$ multilayers functioning at different oxidation times.

more slowly (139 μm at 0.28 μm/min) than those on 5-min-oxidized multilayers. However, cells on 20-min-oxidized multilayers hardly traveled at all (70 μm at 0.12 μm/min) as shortest distances were observed.

4 Conclusions

We have demonstrated an approach for tuning the stiffness of the PEM system by applying the electrochemical treatment. The stiffness of the $(PEI\text{-}Fc/DNA)_{15}$ multilayers could be modulated, ranging from 1.072 to 2.047 MPa. We found that fibroblast cells tended to preferentially attach to a stiffer surface. The stiffness of the multilayers strongly modulated not only the initial cell adhesion and proliferation, but also the cell migration. The present experimental results highlighted, in particular, the key role of electrochemical treatment in improving the mechanical properties of multilayers. Furthermore, our results revealed the effect of the stiffness of stimuli-responsive films on cell adhesion, proliferation, and migration, which will help to provide new insight into the understanding of cell/material interactions.

Acknowledgments: Financial support from the National Natural Science Foundation of China (21174126, 51103126, 51333005, and 21374095), China National Funds for Distinguished Young Scientists 51025312, the National Basic Research Program of China (2011CB606203), Open Project of State Key Laboratory of Supramolecular Structure and Materials (SKLSSM201316), Research Fund for the Doctoral Program of Higher Education of China (20110101110037, 20110101120049, and 20120101130013), the Qianjiang Excellence Project of Zhejiang Province

(2013R10035), and the International Science & Technology Cooperation Program of China (2014DFG52320) is gratefully acknowledged.

References

1. Decher G. Fuzzy nanoassemblies: toward layered polymeric multicomposites. Science 1997;277(5530):1232–7.
2. Schlenoff JB, Decher G. Multilayer thin films: sequential assembly of nanocomposite materials. Wiley VCH: Weinheim, Germany; 2003.
3. De Geest BG, De Koker S, Sukhorukov GB, Kreft O, Parak WJ, Skirtach AG. Polyelectrolyte microcapsules for biomedical applications. Soft Matter. 2009;5(2):282–91.
4. Gribova V, Auzely-Velty R, Picart C. Polyelectrolyte multilayer assemblies on materials surfaces: from cell adhesion to tissue engineering. Chem Mater. 2011;24(5):854–69.
5. Shi F, Liu Z, Wu G, Zhang M, Chen H, Wang Z, Zhang X, Willner I. Surface imprinting in layers-by-layer nanostructured films. Adv Funct Mater. 2007;17(11):1821–7.
6. Shi F, Dong B, Qiu D, Sun J, Wu T, Zhang X. Layer-by-layer self-assembly of reactive polyelectrolytes for robust multilayers patterning. Adv Mater. 2002;14(11):805–9.
7. Louguet S, Rousseau B, Epherre R, Guidolin N, Goglio G, Mornet S. Thermoresponsive polymer brush-functionalized magnetic manganite nanoparticles for remotely triggered drug release. Polym Chem. 2012;3(6):1408–17.
8. Hu X, Wang R, Yue J, Liu S, Xie Z, Jing X. Targeting and antitumor effect of folic acid-labeled polymer – Doxorubicin conjugates with pH-sensitive hydrazone linker. J Mater Chem. 2012;22(26):13303–10.
9. Ren K, Wang L, Ji J, Lin K, Shen J. Construction and deconstruction of PLL/DNA multilayered films for DNA delivery: effect of ionic strength. Colloids Surf B 2005;46(2):63–9.
10. Sortino S. Photoactivated nanomaterials for biomedical release applications. J Mater Chem. 2012;22(2):301–18.
11. Zhai L. Stimuli-responsive polymer films. Chem Soc Rev. 2013;42(17):7148–60.
12. Ramos J, Llarena I, Moya S. Unusual collapse of highly hydrated polyelectrolyte multilayers with the ionic strength. J Polym Sci Pol Chem. 2011;49(11):2346–52.
13. Swiston AJ, Cheng C, Um SH, Irvine DJ, Cohen RE, Rubner MF. Surface functionalization of living cells with multilayer patches. Nano Lett. 2008;8(12):4446–53.
14. Monge C, Saha N, Boudou T, Pózos-Vásquez C, Dulong V, Glinel K. Rigidity-patterned polyelectrolyte films to control myoblast cell adhesion and spatial organization. Adv Funct Mater. 2013;23(27):3432–42.
15. Ma J, Cai P, Qi W, Kong D, Wang H. The layer-by-layer assembly of polyelectrolyte functionalized graphene sheets: a potential tool for biosensing. Colloids Surf A 2013;426:6–11.
16. Iost RM, Crespilho FN. Layer-by-layer self-assembly and electrochemistry: applications in biosensing and bioelectronics. Biosens Bioelectron. 2012;31(1):1–10.
17. Laurent D, Schlenoff JB. Multilayer assemblies of redox polyelectrolytes. Langmuir 1997;13(6):1552–57.
18. Sun Y, Ren K, Zhao Y, Liu X, Chang G, Ji J. Construction of redox-active multilayer film for electrochemically controlled release. Langmuir 2013;29(35):11163–8.
19. Zhu L, Zhou W, Ji J. Ferrocenyl branched poly (ethylene imine) micelles as reductive templates for the preparation of silver nanoparticles. J Nanopart Res. 2010;12(6):2179–87.
20. Schlenoff JB, Laurent D, Ly H, Stepp J. Redox-active polyelectrolyte multilayers. Adv Mater. 1998;10(4):347–9.
21. Liu A, Kashiwagi Y, Anzai J. Polyelectrolyte multilayer films containing ferrocene: effects of polyelectrolyte type and ferrocene contents in the film on the redox properties. Electroanalysis 2003;15(13):1139–42.
22. Fushimi T, Oda A, Ohkita H, Ito S. Fabrication and electrochemical properties of layer-by-layer deposited ultrathin polymer films bearing ferrocene moieties. Thin Solid Films 2005;484 (1–2):318–23.
23. Sato H, Anzai J. Preparation of layer-by-layer thin films composed of DNA and ferrocene-bearing poly(amine)s and their redox properties. Biomacromolecules 2006;7(6):2072–76.
24. Wells R. The role of matrix stiffness in regulating cell behavior. Hepatology 2008;47(4):1394–400.
25. Discher D, Janmey P, Wang Y. Tissue cells feel and respond to the stiffness of their substrate. Science 2005;310(5751):1139–43.
26. Boudou T, Crouzier T, Ren K, Blin G, Picart C. Multiple functionalities of polyelectrolyte multilayer films: new biomedical applications. Adv Mater. 2010;22(4):441–67.
27. Song J, Janczewski D, Ma Y, Hempenius M, Xu J, Vancso GJ. Redox-controlled release of molecular payloads from multilayered organometallic polyelectrolyte films. J Mater Chem B 2013;1(6):828–34.
28. Ando Y, Murai J, Miyashita T, Miyazaki T. Spin dependent tunneling in 80NiFe/LB film with ferrocene and tris(bipyridine) ruthenium derivatives cojunctions. Thin Solid Films 1998; 331(1–2):158–64.
29. Grieshaber D, Voros J, Zambelli T, Ball V, Schaaf P, Voegel JC. Swelling and contraction of ferrocyanide-containing polyelectrolyte multilayers upon application of an electric potential. Langmuir 2008;24(23):13668–76.
30. Tokarev I, Minko S. Stimuli-responsive hydrogel thin films. Soft Matter 2009;5(3):511–24.
31. Sun Y, Ren K, Wang J, Chang G, Ji J. Electrochemically controlled stiffness of multilayers for manipulation of cell adhesion. ACS Appl Mater Int. 2013;5(11):4597–602.
32. Zhu L, Shangguan Y, Sun Y, Ji J, Zheng Q. Rheological properties of redox-responsive, associative ferrocene-modified branched poly(ethylene imine) and its modulation by beta-cyclodextrin and hydrogen peroxide. Soft Matter. 2010;6(21):5541–6.
33. Hodak J, Etchenique R, Calvo EJ, Singhal K, Bartlett PN. Layer-by-layer self-assembly of glucose oxidase with a poly(allylamine) ferrocene redox mediator. Langmuir 1997;13(10):2708–16.
34. Wang Z, Moehwald H, Gao C. Preparation and redox-controlled reversible response of ferrocene-modified poly(allylamine hydrochloride) microcapsules. Langmuir 2011;27(4):1286–91.
35. Kalita G, Sharma S, Wakita K, Umeno M, Hayashi Y, Tanemura M. A photoinduced charge transfer composite of graphene oxide and ferrocene. Phys Chem Chem Phys. 2013;15(4):1271–4.